Supplementary Information of "A Fast 2D MoS_2 Photodetector with Ultralow Contact Resistance"

Wangheng Pan,[a] Anran Wang,[a] Xingguang Wu,[c,d] Xialian Zheng,[b] Hu Chen,[a] Shuchao Qin,[b] Zheng Han,[c,d,e] Siwen Zhao,[*e] Rong Zhang,[a] and Fengqiu Wang[*a]

[a] School of Electronic Science and Engineering, Nanjing University, Nanjing 210093, China. E-mail: fwang@nju.edu.cn

[b] Key Laboratory of Optical Communication Science and Technology of Shandong Province, School of Physical Science and Information Engineering, Liaocheng University, Liaocheng 252059, China.

[c] State Key Laboratory of Quantum Optics and Quantum Optics Devices, Institute of Optoelectronics, Shanxi University, Taiyuan 030006, China.

[d] Collaborative Innovation Center of Extreme Optics, Shanxi University, Taiyuan 030006, China.

[e] Liaoning Academy of Materials, Shenyang 110167, China. E-mail: siwenzhao0126@gmail.com

Supplementary Note 1. The saturation of output curves of the fast MoS_2 photodetector

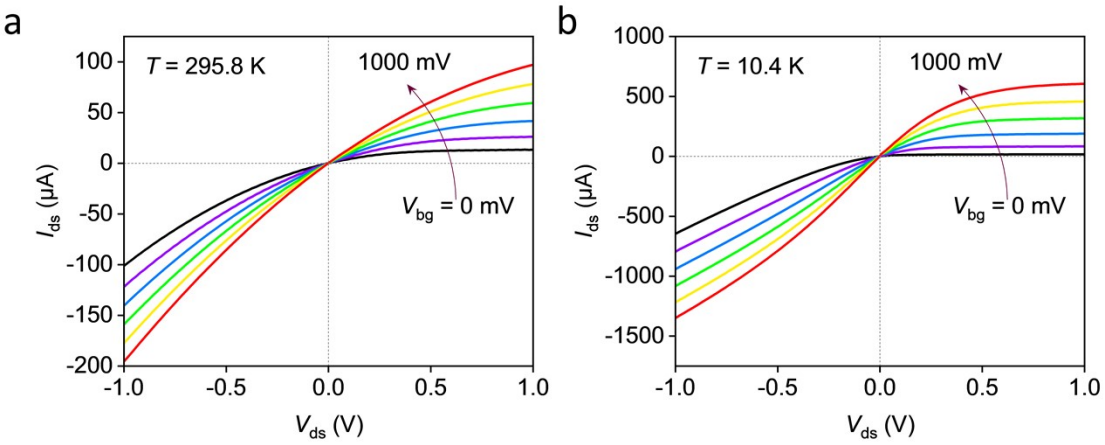

Figure S1 Output curves (I_{ds}-V_{ds}) under different back gate voltages (V_{bg}) at 295.8 K (a) and 10.4 K (b), extended V_{ds}.

At a given gate voltage, the output current tends to saturate as the V_{ds} increases, which leads to an increase in the device's resistance, as shown in Fig. S1a. The saturated current can be attributed to the regulating effect of the gate voltage, since the output curve shows different upper limit of I_{ds} at different V_{bg}. This phenomenon is more pronounced at low temperatures (Fig. S1b), and it can be obtained that the resistance is about 1650 Ω at V_{ds} = 1 V (V_{bg} = 1 V, 10.4 K) and 600 Ω at V_{ds} = 0.1 V (V_{bg} = 1 V, 10.4 K).

Supplementary Note 2. High-resolution temporal response of the fast MoS_2 photodetector with different amplification levels of SR570

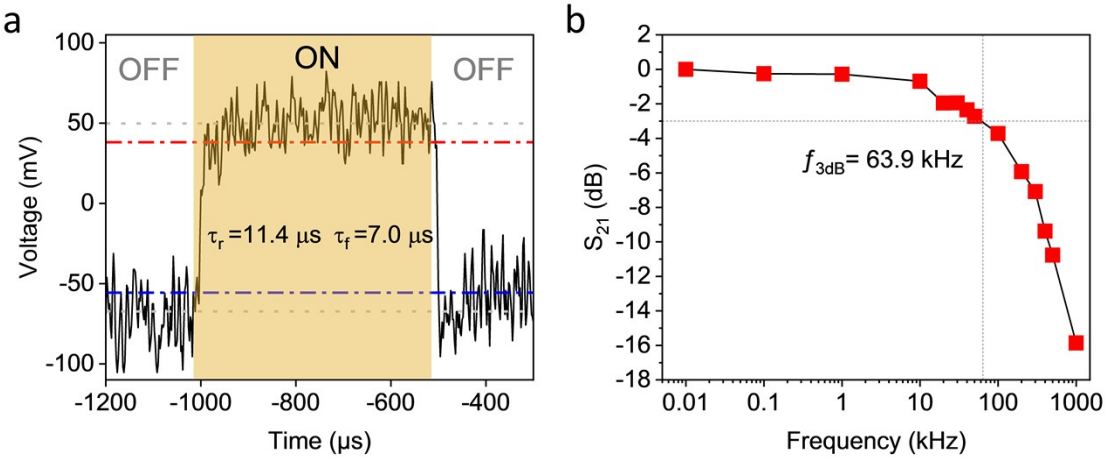

Figure S2 (a) High-resolution temporal response of MoS_2 PDs (Gray dot: on/off steady-state average value. Blue/red dash dot: 10%/90% response intensity.) measured at V_{ds} = 1 V and V_{bg} = 1 V bias, 10.4 K, with 532 nm CW laser power of 20 μW before modulation, modulation frequency: 1000 Hz, 50% duty cycle, 10 μA/V amplification level. (b) Photocurrent gain expressed in dB as a function of the increasing light-modulated frequency, 20 μA/V amplification level (The amplifier will overload when using the 10 μA/V amplification level).

It is noted that the gain/bandwidth characteristics of the transconductance amplifier SR570 is adjustable. Since the amplification level is controlled by the input resistance of amplifier's internal circuit, where a larger resistance corresponds to a larger gain, the output *RC* limitation will be affected. Therefore, if the measurement of our device is already limited by the operating bandwidth of the amplifier, the response rate should be further reduced when switching to a larger amplification level. The experimental results at higher amplification levels of SR570 than that in the main text is shown in Fig. S2, and the obtained response rate of MoS_2 PDs is almost identical. This indicates that our results represent the intrinsic photo-response rate of the device.

Supplementary Note 3. The on/off photoresponse current of the fast MoS_2 photodetector at different wavelengths

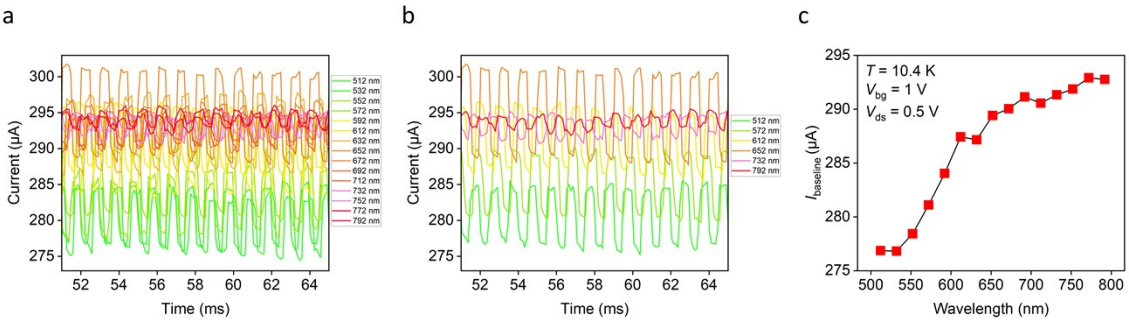

Figure S3 (a) The on/off photoresponse current at different wavelengths (from 512 nm to 792 nm, step: 20 nm) with incident laser power of 15 μW, at 10.4 K. (b) The response current at several representative wavelengths of (a). (c) The photocurrent baseline position at different wavelengths (from 512 nm to 792 nm, step: 20 nm) with incident laser power of 15 μW.

Fig. S3a shows the on/off photoresponse curves at different incident wavelengths, and it can be observed that each current baseline shows obvious downward drift from the dark current (~320 μA, Figure 4). To better show the change of photocurrent baseline, the response curves at several representative wavelengths are shown in Fig. S3b. The photocurrent baseline position extracted from Fig. S3a is shown in Fig. S3c, and the decrease of it is more significant at short wavelengths, which can be attributed to more defective states excited by higher incident photon energies. If the wavelength is further extended to blue and violet light, the photon energy is sufficient to help trapped carriers, which are captured by the mid-gap states, to go over the bandgap and then release, restoring the current baseline to its initial state.

Supplementary Note 4. Mapping of the fast MoS_2 Photodetector's photocurrent distribution

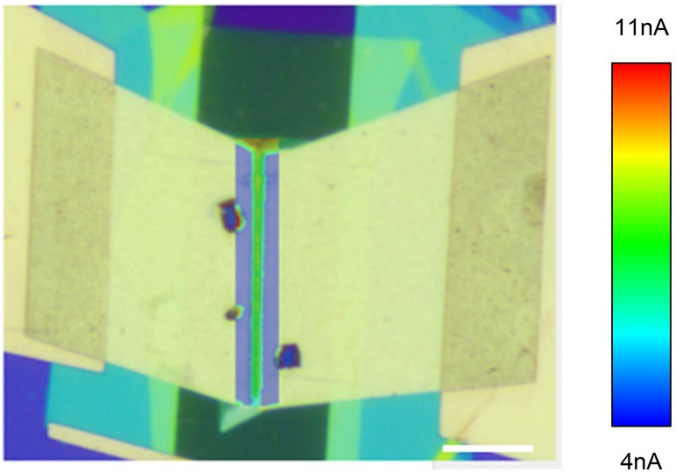

Figure S4 Mapping of device photocurrent distribution, V_{ds} = 0.005 V and V_{bg} = 0 V, room temperature. Scale bar: 10 μm.

To exclude the influence of position on the photocurrent, we scanned the photocurrent distribution in the core area of the device (Fig. S4). According to our proposed mechanism, the application of back-gate voltage will promote the capture of charge carriers by defects. Therefore, the measurements were performed without any back-gate voltage. It can be seen that the device shows uniform positive light response, with the response region only located at the MoS_2 channel area without electrode cover. The positive response exhibited without back gate voltage further indicates the close correlation between back gate and negative response.

Supplementary Note 5. An exemplar response showing characteristic photocurrent transitions of the device.

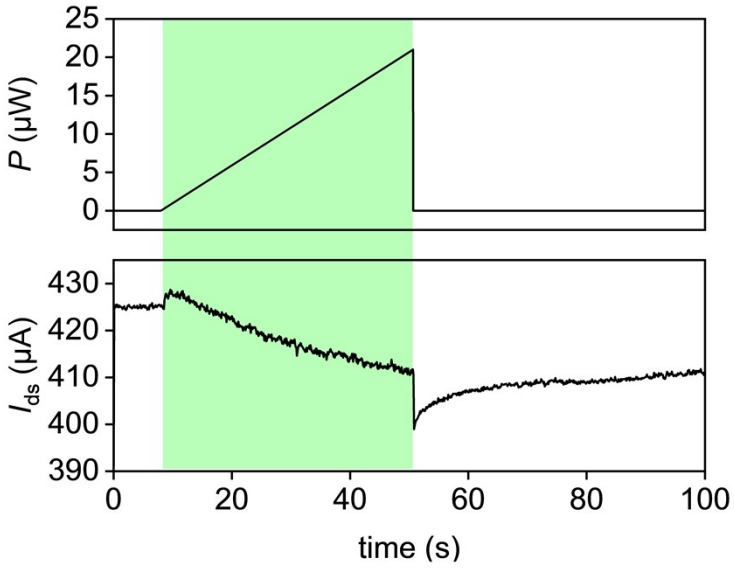

Figure S5 The transitions of device current with light (532 nm CW laser) switching ON and OFF at 10.4 K (V_{bg} = 1 V, V_{ds} = 1 V).

Fig. S5 shows the change of device current with incident light switching ON and OFF under fixed bias and gate voltages. At the moment of illumination, the photocurrent has a positive response. As the illumination time increases (go beyond a few seconds), the current gradually decreases and becomes smaller than the dark current, which is the reason for the negative photoresponse. Under increased light intensity, the photocurrent is seen to continue to decrease and tend to saturate. When the light excitation is turned off, the photocurrent will drop immediately, which is also consistent with normal positive photoresponse. The overall change of device current is as a result of a combined effect of a positive dynamic responses and negative static responses. Then, the subsequent increase in dark current can be attributed to the gradual release of electrons captured by defects. The initial rapid increase of dark current is probably due to the release of trapped electrons in shallower energy levels at the interface. However, as a proportion of the electrons are captured by deeper energy level defect states in BN, they are more difficult to escape and lead to the persistent negative shift of (dark) current.

Supplementary Note 6. Measuring the capacitance of the fast MoS_2 photodetector

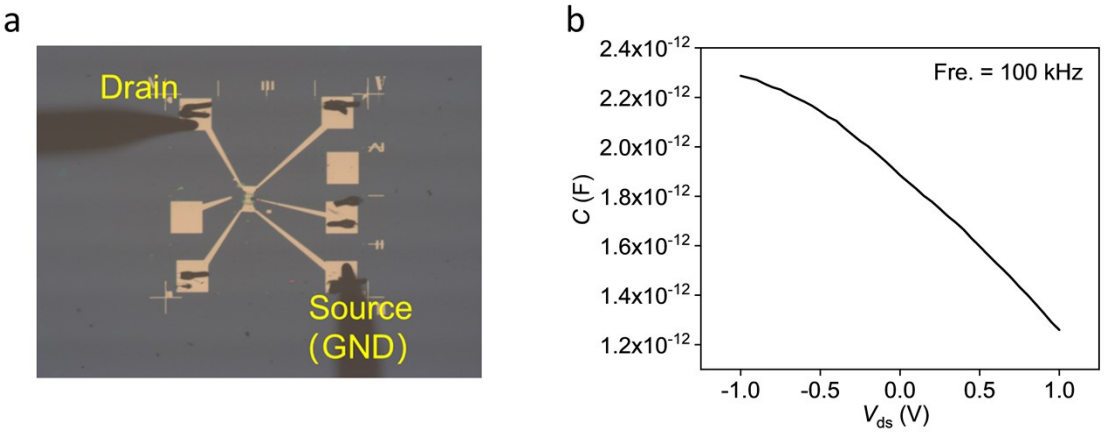

Figure S6 (a) Optical image of the capacitance test. (b) Source drain capacitance under different V_{ds}, fixing the frequency of 100 kHz, room temperature.

Fig. S6a shows the optical image of the PDs under capacitance test. As shown in Fig. S6b, the source-drain capacitance of the PDs is of several pF. By fixing the frequency of the *C*-*V* tester, it can be observed that the V_{ds} has an approximately linear sub-pF level regulation effect on capacitance. The capacitance is 1.26 pF (at V_{ds} = 1 V and V_{bg} = 0 V) at room temperature. Combined with the results shown in Fig. 5a, this capacitance value will not be significantly affected by temperature, causing trivial influence on the *RC* limitation of the device.

Supplementary Note 7. Noise current spectral density of the fast MoS_2 photodetector

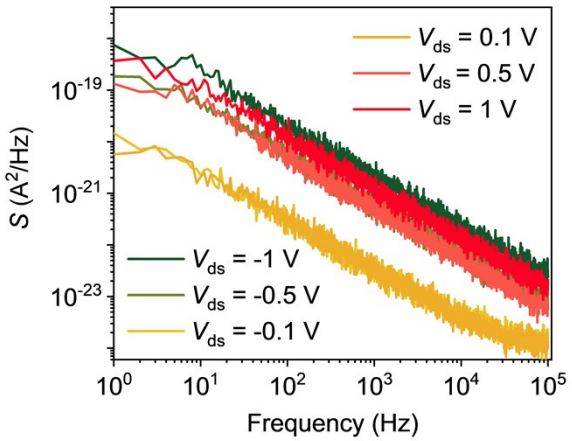

Figure S7 Noise current spectral density under different V_{ds} with V_{bg} = 0 V, room temperature.

Fig. S7 shows the noise current spectral density at a fixed V_{bg} of 0 V under different V_{ds}. It can be seen that the noise increases with the absolute value of V_{ds} increases. The increased noise mainly comes from flicker noise, while the shot noise can be almost ignored.